Physical Properties of III-Antiminodes — a First Principles Study

To cite this article: Rashid Ahmed *et al* 2009 *Commun. Theor. Phys.* **52** 527

View the article online for updates and enhancements.

Physical Properties of III-Antiminodes — a First Principles Study

Rashid Ahmed,[1,*] Fazal-e-Aleem,[1] S. Javad Hashemifar,[2] Haris Rashid,[1] and H. Akbarzadeh[2]

[1]Centre for High Energy Physics University of the Punjab, Lahore-54590-Pakistan

[2]Department of Physics, Isfahan University of Technology, 841546 Isfahan, Iran

Abstract *A comprehensive first principles study of III-Antimonide binary compounds is hardly found in literature. We report a broad study of structural and electronic properties of boron antimonide (BSb), aluminium antimonide (AlSb), gallium antimonide (GaSb) and indium antimonide (InSb) in zincblende phase based on density functional theory (DFT). Our calculations are based on Full-Potential Linearized Augmented Plane wave plus local orbitals (FP-L(APW+lo)) method. Different forms of exchange-correlation energy functional and corresponding potential are employed for structural and electronic properties. Our computed results for lattice parameters, bulk moduli, their pressure derivatives, and cohesive energy are consistent with the available experimental data. Boron antimonide is found to be the hardest compound of this group. For band structure calculations, in addition to LDA and GGA, we used GGA-EV, an approximation employed by Engel and Vosko. The band gap results with GGA-EV are of significant improvement over the earlier work.*

1 Introduction

III-Antimonide binary compounds are common-anion family of III-V semiconductors. At ambient conditions, these binary compounds crystallize in the zincblende structure. Boron antimonide (BSb) and Aluminum antimonide (AlSb) are indirect band gap semiconductors, while Gallium antimonide (GaSb) and Indium antimonide (InSb) are direct band gap semiconductors. Although a piecemeal explanation of some of the physical parameters for this family is available,[1−32] a comprehensive picture is elusive.

In recent years, III-Antimonides have attracted more interest due to their potential applications in rechargeable lithium batteries as anode materials.[15,23−30] Boron Antimonide (like Boron Arsanide and Boron Phosphide) shows strong covalent character and exhibits an unusual behavior due to small core and absence of "p" electrons in boron atom compared to other III-V compounds.[9] It makes this compound a potential material for high temperature electronic and optical applications. Similarly, GaSb is a good candidate for thermo-photovoltaic cells for systems with low radiator temperature, as its cell technology is rather straightforward resulting in higher efficiency than Si thermo-photovoltaic cells.[31] Antimonide compounds, due to their high mobility, are therefore well-known for advanced device applications.[32]

In view of their importance as "base material" for many state of the art devices, it is important to know different properties of these semiconductor compounds. Within the frame work of density functional theory (DFT),[33,34] very little work using full-potential linearised augmented plane wave (FP-LAPW) method and pseudo-potential methods[35] is reported. Generally, theoretical work is based on Hartree–Fock (HF) method.

Exchange correlation energy functional (and corresponding potential) have a key position in DFT based total energy calculations. Studies with LDA (local-density approximation)[36] or GGA (generalized gradient approximation)[37] for exchange correlation energy functional and corresponding potential give lower values of band gap energy. We therefore use GGA-EV, another form of exchange correlation functional proposed by Engel and Vosko.[38] This approximation gives better results for the electronic properties of different solids.[39−47] In this paper, we give broad theoretical description for electronic (band gap) and structural (lattice parameters, cohesive energy, bulk modulus, pressure derivative) properties for III-antimonides using FP-LAPW method with LDA, GGA, and GGA-EV. Results provide useful and fundamental understanding of III-Antimonide binary compounds.

2 Computational Methodology

In our computations, we distinguish the core electrons of B $(1s^2)$, Al $(1s^22s^22p^6)$, Ga $(1s^22s^2\ 2p^63s^23p^6)$, In $(1s^22s^22p^63s^23p^63d^{10}4s^24p^6)$, Sb $(1s^22s^22p^63s^23p^63d^{10}4s^24p^6)$, and the valence electrons of B $(2s^22p^1)$, Al $(3s^23p^1)$, Ga $(3d^{10}4s^24p^1)$, In $(4d^{10}5s^25p^1)$ and Sb $(4d^{10}5s^25p^3)$. The zincblende structure consists of two interpenetrating FCC sub-lattice at positions R $(0, 0, 0)$ and $(1/4, 1/4, 1/4)$.[1]

We used FP-L(APW+lo) method embedded in WIEN2k package.[48,49] In this technique, unit cell is di-

vided into two regions: non-overlapping muffin-tin (MT) spheres centered on atomic nuclei and the remaining interstitial region, and no shape approximation for potential is used. In these two regions, Kohn–Sham wave functions, charge density and potential are expanded differently. In the interstitial region, plane waves are used for expansion while inside MT spheres, basis functions are linear combination of radial solutions to the single particle Schrödinger equation and their energy derivatives, multiplied by the spherical harmonics. The charge density and potential are expanded into lattice harmonics inside MT spheres and as a Fourier series in the remaining space. Core states are treated taking into account full relativistic effects while valence states are treated within scalar relativistic approximation.[44−49]

While computing, the maximum quantum number $l_{\max}$, for the expansion of atomic wave functions inside the MT spheres, was taken equal to 10 and the energy cutoff for plane wave expansion of wave functions in the interstitial region was chosen to be $K_{\max} = 8.0/R_{MT}$. Fourier expanded charge density was truncated at $G_{\max} = 14$ (Ryd)$^{1/2}$. The R_{MT} values for B, Al, Ga, In, and Sb are taken as 1.5 a.u, 2.0 a.u., 2.1 a.u, 2.4 a.u, and 2.3 a.u.. Reciprocal space integration was performed using an improved tetrahedron method[50] with a mesh of 30 special k-points in the irreducible wedge of the Brillion zone.

3 Results and Discussions

3.1 *Structural Properties*

To compute the structural properties of BSb, AlSb, GaSb, and InSb, for the exchange-correlation energy of electrons, LDA and GGA were used. Total energy of primitive unit cell at different volumes is calculated over a range ±10% around experimental volumes for III-Antimonides. By fitting the Murnaghan equation of state[51] to the obtained energy-volume data, equilibrium lattice parameters, bulk moduli, its pressure derivative and cohesive energy were calculated (Table 1). These results are reported along with available experimental data and theoretical computations of other authors. As a sample, energy-volume curve of AlSb within LDA is shown in Fig. 1.

From Table 1, it may be observed that our calculated lattice parameters compared with the experiment are slightly underestimated within LDA and overestimated within GGA. However, all computations for lattice parameters agree with the experimental results within 1–2 %. It may be noted that results obtained with Hartree–Fock method are higher than experimental measurements.

Bulk modulus is a fundamental property. It determines hardness of cubic crystals and has an important part in establishing stability criteria. Calculated bulk moduli are given in Table 1. Results with LDA are in agreement with experimental measurements whereas GGA underestimates experiment. BAs compound give

much higher bulk modulus in this family, which is due to the strong covalent bonding between B and Sb. Results from HF for bulk modulus overestimate the experimental data. Pressure derivative of bulk modulus, has also been calculated and is given in Table 1.
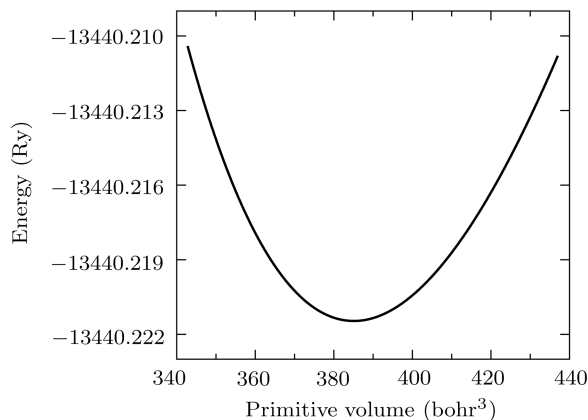
Fig. 1 Total energy vs. primitive cell volume for zb-AlSb within LDA.

Cohesive energy, the difference between total energy of isolated atoms and crystal unit cell, was also calculated for III-Antimonides. In Table 1, we present calculated cohesive energies using LDA and GGA. Consistent with the general belief, we observe that LDA over-binds cohesive energies and gives higher values than the experimental data while GGA corrects this over-binding and provides better agreement. Calculated cohesive energies with GGA are therefore more reliable. No earlier results for cohesive energy for III-Antimonides, using density functional theory are available. Cohesive energy values calculated using HF method are significantly lower than the experimental data.

3.2 *Electronic Properties*

We used experimental values of lattice parameters (except for BSb where no experimental value is available) for consistent study of electronic band structure using different approximations of exchange-correlation potential. The Kohn-Sham eigenvalues were calculated with LDA, GGA, and GGA-EV by FP-L (APW+lo) method along some high symmetry directions in the Brillion zone. The calculated values for band gap, E_g, are given in Table 2 along with other available theoretical predictions and experimental data.

It is observed that LDA and GGA give essentially similar band structure and close band gaps values while with GGA-EV the unoccupied bands are shifted upward, leading to an enhanced band gap. The shape of band structure and character of band gap is similar in all approximations and the main difference is in the numerical values. Observed band gap enhancement in GGA-EV usually compensates the problem of insulator and semiconductor band gap underestimation in LDA and GGA.

Table 1 The lattice parameter (a), bulk modulus (B), its pressure derivative (B') and cohesive energy per unit cell ($E_{\rm Coh}$) of BSb, AlSb, GaSb, and InSb compounds.

Compounds	Method	a (Å)	B (GPa)	B'	$E_{\rm Coh}$ (eV)
BSb					
Present work	FP-LDA	5.191	111	4.36	10.26
	FP-GGA	5.279	096	4.55	08.48
Experiment	-	-	-	-	-
Other calculations	PP-LDA	5.12 [7]	115 [7]	5.28 [7]	-
	PP-LDA	5.156 [9]	108 [9]	4.03 [9]	-
	FP-GGA	5.252 [10]	103 [10]	3.89 [10]	-
	PP-LDA	5.177 [13]	110 [13]	4.24 [13]	-
	FP-LDA	5.201 [14]	116 [14]	4.16 [14]	-
	FP-GGA	5.278 [14]	100 [14]	4.40 [14]	-
	FP-GGA	5.252 [17]	103 [17]	-	-
	PP-LDA	5.201 [19]	109 [19]	4.00 [19]	-
AlSb					
Present work	FP-LDA	6.111	56	4.52	8.08
	FP-GGA	6.230	49	4.28	6.68
Experiment	-	6.135 [1]	58 [1]	-	6.60 [1]
-	-	6.096 [11]	-	-	-
Other calculations	PP-LDA	6.09 [12]	56 [12]	4.36 [12]	-
	PP-LDA	6.08 [15]	-	-	-
	HF	6.22 [2]	61 [2]	-	4.00 [2]
	HF	-	-	-	0.146[5]
	HF	6.261 [6]	65 [6]	-	-
GaSb					
Present work	FP-LDA	6.053	54	4.26	7.43
	FP-GGA	6.219	45	4.02	5.81
Experiment	-	6.118 [1]	56 [1]	-	6.00 [1]
Other calculations	LMTO-LDA	5.939 [4]	80 [4]	-	-
	PP-LDA	5.981 [12]	57 [12]	4.66 [12]	-
	PP-LDA	5.95 [15]	-	-	-
	HF	[2]	59 [2]	-	3.00 [2]
	HF	-	-	-	0.109[5]
	HF	6.212 [6]	63 [6]	-	-
InSb					
Present work	FP-LDA	6.456	46	4.51	6.97
	FP-GGA	6.640	37	4.43	5.39
Experiment	-	6.478 [1]	46 [1]	-	5.60 [1]
Other calculations	PP-LDA	6.346 [12]	48 [12]	4.69 [12]	-
	PP-LDA	6.30 [15]	-	-	-
	HF	6.56 [2]	50 [2]	-	2.80 [2]
	HF	-	-	-	0.117[5]
	HF	6.593 [6]	58 [6]	-	-
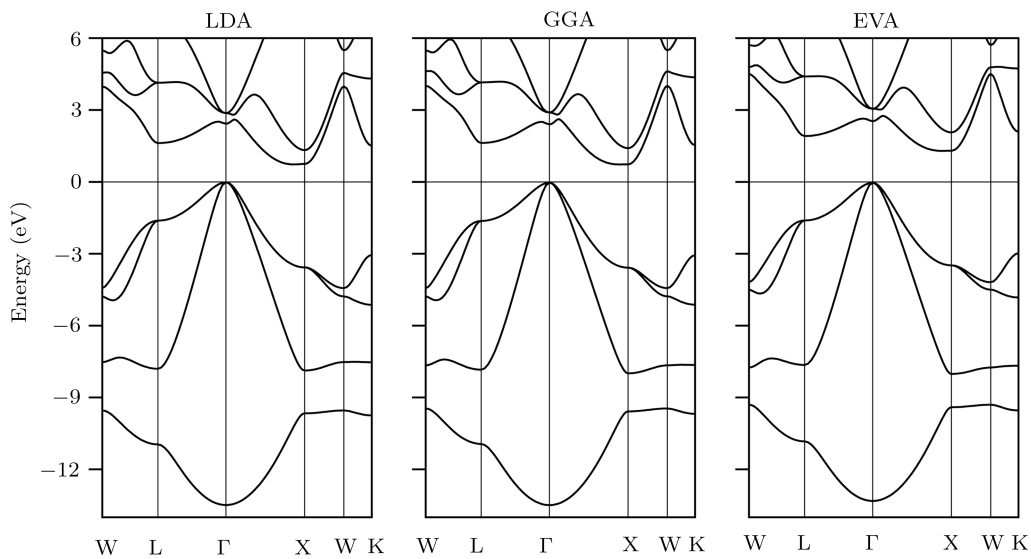
Fig. 2 Band structure of zb-BSb within LDA, GGA, and EVA.

Table 2   The energy band gap (Eg) properties of BSb, AlSb, GaSb, and InSb. XC: Exchange correlation approximation.

| Compounds	Methods	XC	E_g (eV)	Type of band-gap
BSb				
Present work	FP-LAPW	LDA	0.751	Indirect (Γ-$\Delta_{\min}$)
		GGA	0.763	Indirect (Γ-$\Delta_{\min}$)
		EVA	1.334	Indirect (Γ-$\Delta_{\min}$)
Experiment		-	0.51 [18]	Indirect (Γ-$\Delta_{\min}$)
Other calculations	PP-PW	LDA LDA	0.527 [7]	Indirect (Γ-$\Delta_{\min}$)
	PP-PW	LDA	0.62 [9]	Indirect (Γ-$\Delta_{\min}$)
	FP-LAPW	GGA	0.75 [10]	Indirect (Γ-$\Delta_{\min}$)
	FP-LAPW	LDA	0.56 [14]	Indirect (Γ-$\Delta_{\min}$)
	FP-LAPW	GGA	0.71 [14]	Indirect (Γ-$\Delta_{\min}$)
	PP-PW	LDA	[18] [18]	Indirect (Γ-$\Delta_{\min}$)
AlSb				
Present work	FP-LAPW	LDA	1.141	Indirect (Γ-$\Delta_{\min}$)
		GGA	1.214	Indirect (Γ-$\Delta_{\min}$)
		EVA	1.835	Indirect (Γ-$\Delta_{\min}$)
Experiment		-	1.686 [1]	
Other calculations	PP-PW	LDA	1.67 [12]	Indirect (Γ-$\Delta_{\min}$)
GaSb				
Present work	FP-LAPW	LDA	0.000	Direct (Γ-Γ)
		GGA	0.028	Direct (Γ-Γ)
Experiment	-	EVA	0.361	Direct (Γ-Γ)
		-	0.670 [3]	Direct (Γ-Γ)
-	-	-	0.7 [11]	Direct (Γ-Γ)
Other calculations	LMTO	LDA	0.470 [4]	Direct (Γ-Γ)
	PP-PW	LDA	0.547 [12]	Direct (Γ-Γ)
InSb				
Present work	FP-LAPW	LDA	0.000	Direct (Γ-Γ)
		GGA	0.000	Direct (Γ-Γ)
		EVA	0.200	Direct (Γ-Γ)
Experiment	-	-	0.2 [11]	Direct (Γ-Γ)
-	-	-	0.25 [16]	Direct (Γ-Γ)
Other calculations	FP-LAPW	LDA	-0.72 [8]	Direct (Γ-Γ)
	PP-PW	LDA	0.213 [12]	Direct (Γ-Γ)
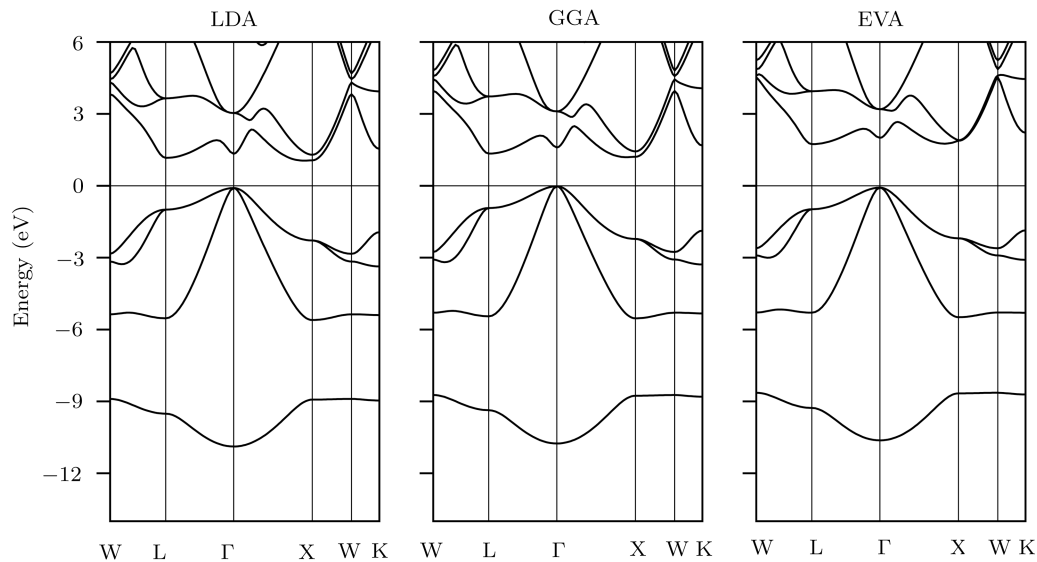
Fig. 3   Band structure of zb-AlSb within LDA, GGA, and EVA.

According to calculated band structure for BSb and AlSb (Figs. 2 and 3), minima of camel's back shape conduction band is found close to X along a Δ-line and maxima of valence band at Γ, leading to an indirect band gap at Γ-Δ_{min} for these compounds. Our calculated band gap values with GGA are in agreement with previous first principles computations. However, for LDA, we get a higher (for BSb) and lower (for AlSb) band gap value compared to other theoretical results (Table 2). In case of BSb, it may be because band structure calculations were performed using theoretical lattice parameters due to non-availability of experimental lattice constants. As expected, our results using GGA-EV are higher than LDA and GGA. For BSb, we observed that unlike general trend of LDA and GGA, computed band gap values are consistently higher than the experimental value. This indicates that either the experimental value of band gap needs to be measured again or some very unusual phenomena is taking place. Therefore further experimental work is important and needs a through probe for BSb.
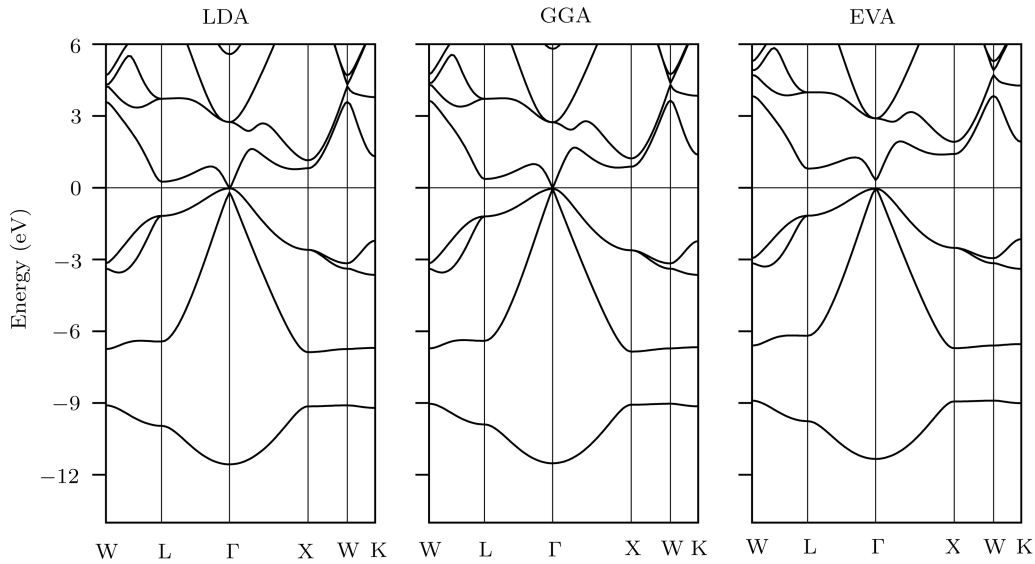
Fig. 4 Band structure of zb-GaSb within LDA, GGA, and EVA.
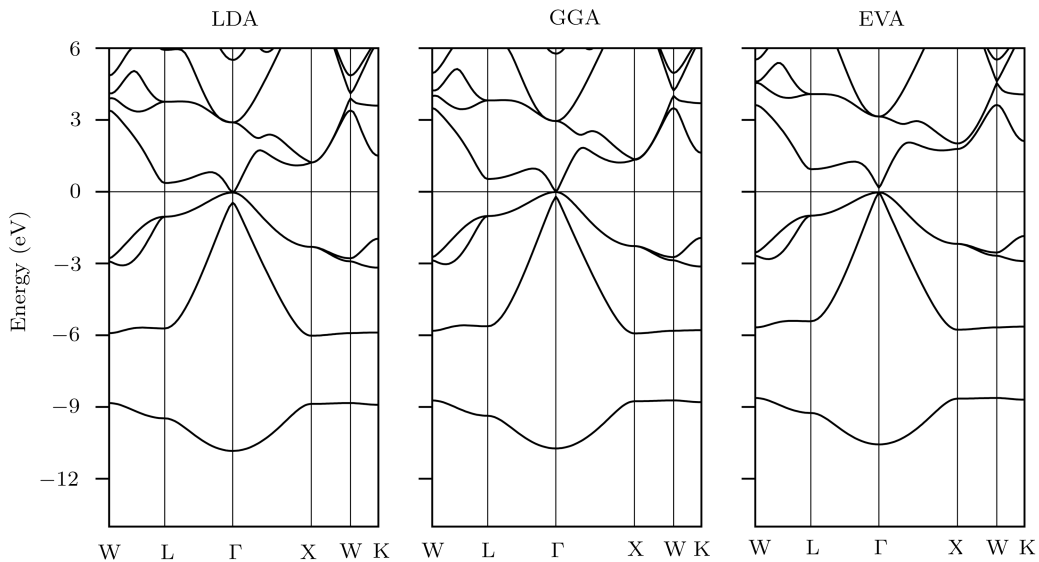
Fig. 5 Band structure of zb-InSb within LDA, GGA, and EVA.

Calculated results indicate that GaSb and InSb (Figs. 4 and 5) have direct band gaps at Γ. Predicted band gap within LDA and GGA are near zero, indicating a metal like behavior of these two compounds (which is not true). It may be due to the choice of "exchange correlation functional" in LDA and GGA that were not able to determine precise band gap of semiconductors. However, GGA-EV improves theoretical results in comparison with the measured values. Predicted band gap for InSb with GGA-EV (0.206 eV at Γ) is consistent with the experimental value while for GaSb there is an underestimation. The qualitative nature of our calculated electronic band gap is similar to earlier results. The pseudo potential calculations with LDA[12] for InSb give consistent value of band gap to experiment that is due to some manual (non-first-principle) adjustments of the pseudo potential.

The general features to note are:

(i) Our work provides a broad theoretical study of structural and electronic properties of III-Antimonides.

(ii) Cohesive energy has not been calculated using density functional theory. Similarly, lattice parameters and bulk moduli (except for BSb) have not been calculated using GGA. In addition, electronic band gap for AlSb, GaSb, and InSb has not been calculated using GGA. Our computations include all these important calculations.

(iii) A detailed study of electronic band structure calculations establishes that GGA-EV gives better results.

(iv) Calculations based on LDA and GGA for all III-Antimonides give lower values for the band gap compared with GGA-EV that optimizes the exchange correlation potential and yields better band splitting.

4 Conclusion

Structural and electronic properties of III-antimonides were studied using FP-LAPW method based on density functional theory. Structural properties obtained with LDA and GGA are in good agreement with the experimental data. In case of band structure both LDA and GGA give rather similar band gap values that are considerably lower than experiment while GGA-EV improves the results.

Acknowledgments

References

[1] R.W.G. Wyckoff, *Crystal Structures*, 2nd Edition, Krieger, Malabar (1986); O. Madelung, *Semiconductors: Data Handbook*, Springer, Berlin (2004); O. Madelung, *Numerical data and Functional Relationships in Science and Technology*, Springer, Berlin (1982); http://cst-www.nrl.navy.mil/lattice/.

[2] M. Causa, R. Dovesi, and C. Roetti, Phys. Rev. B **43** (1991) 11937.

[3] R.C. Weast, D.R. Lide, M.J. Astle, and W.H. Beyer, *CRC Handbook of Chemistry and Physics*, 70th edition edited by CRC, Boca Ratom, Florida (1990).

[4] B.K. Agrawal, P.S. Yadav, S. Kumar, and S. Agrawal, Phys. Rev. B **52** (1995) 4896.

[5] B. Paulus, P. Fulde, and H. Stoll, Phys. Rev. B **54** (1996) 2556.

[6] S. Kalvoda, B. Paulus, P. Fulde, and H. Stoll, Phys. Rev. B **55** (1997) 4027.

[7] M. Ferhat, B. Bouhafs, A. Zaoui, and H. Aourag, J. Phys.: Condens. Matter **10** (1998) 7995.

[8] R. Ashi, W. Mannstadt, and A.J. Freeman, Phys. Rev. **59** (1999) 7486.

[9] B. Bouhafs, H. Aourag, and M. Cartier, J. Phys. Matter **12** (2000) 5655.

[10] A. Zaoui and F. El. Haj Hassan, J. Phys.: Condens. Matter **13** (2001) 253.

[11] I. Vurgaftman, J.R. Meyer, and L.R. Ram-Mohan, J. Appl. Phys. **89** (2001) 5815; references therein; A. Mujica, Angel Rubio, A. Munoz, and R.J. Needs, Rev. Mod. Phys. **75** (2003) 863; references therein; G.J. Ackland, Rep. Prog. Phys. **64** (2001) 483; references therein.

[12] S.Q. Wang and H.Q. Ye, J. Phys.: Condens. Matter **14** (2002) 9579.

[13] S.Q. Wang and H.Q. Ye, Phys. Rev. B **66** (2002) 235111.

[14] H. Meradji, S. Drablia, S. Ghemid, H. Belkhir, B. Bouhafs, and A. Tadjer, Phys. Stat. Sol. (**b**) (2004) 1–5 / **DOI** 10.1002/pssb.200302064.

[15] Hou Zhu-Feng, Zhu Zi-Zhong, Huang Mei-Chum, and Yang Yong, Phys. Chem. Commun. **6(12)** (2003) 47.

[16] Alan Owens and A. Peacock, Nuclear Instruments and Methods in Physics Research A **531** (2004) 18.

[17] F. El. Haj Hassan1, H. Akbarzadeh, and M. Zoaeter, J. Phys.: Condens. Matter **16** (2004) 293.

[18] S. Hussain, S. Dalui, R.K. Roy, and A.K. Pal, J. Phys. D: Appl. Phys. **39** (2006) 2053.

[19] D. Touat, M. Ferhat, and A. Zaoui, J. Phys.: Condens. Matter **18** (2006) 3647.

[20] C. Molteni, L. Colombo, and L. Miglio, J. Phys.: Condens. Matter **6** (1994) 5255.

[21] P. Carrier and Su-H. Wei, Phys. Rev. B **70** (2004) 035212.

[22] C.B. Geller, W. Wolf, S. Picozzi, A. Continenza, R. Asahi, W. Mannstadt, A.J. Freeman, and E. Wimmer, Appl. Phys. Lett. **79** (2001) 368.

[23] J.T. Vaughey, J.O. Hara, and M.M. Thackeray, Electrochem. Solid State Lett. **3** (2000) 13.

[24] J.T. Vaughey, C.S. Johnson, A.J. Kropf, R. Benedek, M.M. Thackeray, H. Tostmann, T. Sarakonsri, S. Hackney, L. Fransson, K. Edström, and J.O. Thomas, J. Power Sources **97-98** (2001) 194.

[25] A.J. Kropf, H. Tostmann, C.S. Johnson, J.T. Vaughey, and M.M. Thackeray, Electrochem. Commun. **3** (2001) 244.

[26] C.S. Johnson, J.T. Vaughey, M.M. Thackeray, T. Sarakonsri, S.A. Hackney, L. Fransson, K. Edstrom, and J.O. Thomas, Electrochem. Commun. **2** (2000) 595.

[27] K.C. Hewitt, L.Y. Beaulieu, and J.R. Dahn, J. Electrochem. Soc. **148**(5) (2001) A402.

[28] R. Benedek, J.T. Vaughey, M.M. Thackeray, L.H. Yang, and R. Prasad, J. Power Sources **97-98** (2001) 201.

[29] R.A. Huggins, in *Handbook of Battery Materials*, ed. J.O. Besenhard, Wiley-VCH, Wienheim (1999) p. 359.

[30] M. Wachtler, M. Winter, and J.O. Besenhard, J. Power Sources **105** (2002) 151.

[31] C.A. Wang, *Antimony Based III-V Thermophotovoltaic Devices*, The Sixth Conf. on "Thermophotovoltaic Generation of Electricity", Freiburg (2004) (http://www.osti.gov/bridge/servlets/purl/836453-aGjhKb/native/836453.pdf); and references therein.

[32] C.R. Bolognesi and D.H. Chow, IEEE Electron Device Lett. **17** (1996) 534.

[33] P. Hohenberg and W. Kohn, Phys. Rev. **136** (1964) 864.

[34] W. Kohn and L.J. Sham, Phys. Rev. A **140** (1965) 1133.

[35] W.E. Pickett, Comput. Phys. Rep. **9** (1989) 117.

[36] J.P. Perdew and Y. Wang, Phys. Rev. B **45** (1992) 13244.

[37] Perdew, K. Burke, and M. Emzerhof, Phys. Rev. Lett. **77** (1996) 3865.

[38] E. Engel and S.H. Vosko, Phys. Rev. B **47** (1993) 13164.

[39] P. Dufek, P. Blaha, and K. Schwarz, Phys. Rev. B **50** (1994) 7279.

[40] C. Persson, R. Ahuja, and B. Johansson, Phys. Rev. B **64** (2001) 033201.

[41] A. Mokhatari and H. Akbarzadeh, Phyisca B **324** (2002) 305.

[42] A. Mokhatari and H. Akbarzadeh, Physica B **337** (2003) 122.

[43] A. Mokhtari and H. Akbarzadeh, J. Phys.: Condens. Matter **16** (2004) 6063.

[44] R. Ahmed, H. Akbarzadeh, and Fazal-e-Aleem, Physica B **370** (2005) 52.

[45] F. El Haj Hassan and H. Akbarzadeh, Materials Science and Engineering B **121** (2005) 170.

[46] R. Ahmed, *et al.*, Comput. Mater. Sci. **39** (2007) 580; B. Amrani, R. Ahmed, and F. El Haj Hassan, Comput. Mater. Sci. **40** (2007) 66; R. Ahmed, *et al.*, Physica B **400** (2007) 297; R. Ahmed, *et al.*, Physica B **403** (2008) 1876.

[47] A. Bouhemadou, R. Khenata, F. Zegrar, M. Sahnoun, H. Baltache, and A.H. Reshak, Comput. Mater. Sci. **38** (2006) 263.

[48] G.K.H. Madsen, P. Blaha, K. Schwarz, E. Sjostedt, and L. Nordstrom, Phys. Rev. B **64** (2001) 195134; P. Blaha, K. Schwarz, G.K.H. Madsen, D. Kvasnicka, and J. Luitz, *WIEN2k, An Augmented Plane Wave + Local Orbitals Program for Calculating Crystal Properties*, Karlheinz Schwarz, Techn. Universität Wien, Austria (2001); ISBN 3-9501031-1-2; K. Schwarz, P. Blaha, and G.K.H. Madsen, *Electronic Structure Calculations of Solids Using the WIEN2k Package for Material Sciences*, Comp. Phys. Commun. **147** (2002) 71.

[49] K. Schwarz and P. Blaha, *Quantum Mechanical Computations at the Atomic Scale for Material Sciences*, WCCM V, Vienna (2002); K. Schwarz and P. Blaha, Comput. Mat. Sci. **28** (2003) 259; http://www.wien2k.at.

[50] H.J. Monkhorst and J.D. Pack, Phys. Rev. B **13** (1976) 5188.

[51] F.D. Murnaghan, "The Compressibility of Media under Extreme Pressures", in *Proceedings of the National Academy of Sciences*, Washington, DC 20418 USA Vol. **30** (1944) p. 244.